Title: Neutrophil-epithelial interactions augment infectivity and pro-inflammatory responses to SARS-CoV-2 infection

Author List: Calvert BA[1], Quiroz EJ[1,2], Lorenzana Z[1], Doan, N[1], Kim S[4], Senger CN[1,2], Wallace WD[5], Salomon MP[6], Henley JE[6], and Ryan AL[1,2*#]

Author Affiliations:

[1]Hastings Center for Pulmonary Research, Division of Pulmonary, Critical Care and Sleep Medicine, Department of Medicine, University of Southern California, Los Angeles, CA, USA

[2]Department of Stem Cell Biology and Regenerative Medicine, University of Southern California, Los Angeles, CA, USA

[3]CFFT Research Laboratory, Cystic Fibrosis Foundation Therapeutics, Lexington, MA, USA

[4]The Salk Institute of Biological Studies, 10010 North Torey Pines Road, La Jolla, Ca, USA

[5]Department of Pathology, University of Southern California, Los Angeles, CA, USA

[6]Department of Medicine, University of Southern California, Los Angeles, CA, USA

Contact Information:

*Corresponding Author and Lead Contact

[#]Previously known as Amy L Firth

Amy L Ryan, PhD

Assistant Professor of Medicine

Hastings Center for Pulmonary Research

Division of Pulmonary, Critical Care and Sleep Medicine, Department of Medicine

Department of Stem Cell Biology and Regenerative Medicine

HMR 712

University of Southern California

Los Angeles, CA 90089

E-mail: amy.firth@med.usc.edu

Tel: 323 442 1833

Highlights:

- We have developed a model to study neutrophil-epithelial interactions which better reflects the *in vivo* situation than monocultures
- Neutrophils significantly augment SARS-CoV-2 mediated, pro-inflammatory cytokine release from the epithelium indicating a key interaction
- SARS-CoV-2 infection leads to a polarized inflammatory response in differentiated airway epithelium
- Disruption of the epithelial barrier via addition of neutrophils or cytokines leads to increased infection
- Study reveals a key role for neutrophil-epithelial interactions in determining outcome/infectivity

Summary: In response to viral infection, neutrophils release inflammatory mediators as part of the innate immune response, contributing to pathogen clearance through virus internalization and killing. Pre-existing co-morbidities, correlating to incidence of severe COVID-19, are associated with chronic airway neutrophilia and examination of COVID-19 lung tissue revealed a series of epithelial pathologies associated with infiltration and activation of neutrophils. To determine the impact of neutrophil-epithelial interactions on the infectivity and inflammatory response to SARS-CoV-2 infection, we developed a co-culture model of airway neutrophilia. We discovered that SARS-CoV-2 infection of the airway epithelium alone does not result in a notable release of pro-inflammatory cytokines, however in the presence of neutrophils, the inflammatory response is both polarized and significantly augmented, epithelial barrier integrity in impaired and viral load of the airway epithelium increased. This study reveals a key role for neutrophil-epithelial interactions in determining inflammation, infectivity, and outcomes in response to SARS-CoV-2 infection.

Keywords: Airway Epithelium, Cell-Cell Interactions, COVID-19, Cytokines, Inflammation, Interferon, Neutrophils, Tissue Remodeling, Viral Infection.

Introduction: Novel coronavirus infectious disease, COVID-19, is caused by the severe acute respiratory distress syndrome related coronavirus 2, SARS-CoV-2 (Guan et al., 2020; Wu and McGoogan, 2020). While COVID-19 is associated with high hospitalization and mortality rates, a substantial proportion of the population is asymptomatic or only experiences mild symptoms. In response to viral infection neutrophils are the first and predominant immune cells recruited to the respiratory tract (Pechous, 2017). Neutrophils release inflammatory mediators as part of the innate immune response and contribute to pathogen clearance through virus internalization and killing (Grommes and Soehnlein, 2011). While the protective versus pathological role of neutrophils in the airways during viral response is poorly understood, it has been shown that the number of neutrophils in the lower respiratory tract correlates to disease severity and is an early marker for COVID-19 (Munoz-Fontela et al., 2020; Song et al., 2020; Zhang et al., 2020a). Infiltration of neutrophils is also characteristic of other lung diseases associated with chronic infection and inflammation, such as asthma, chronic obstructive pulmonary disease (COPD) and cystic fibrosis (CF). All of these respiratory diseases have been associated with an increased risk of contracting severe COVID-19 (Aveyard et al., 2021). Evaluating the relationship between SARS-CoV-2 infection and neutrophilia may provide critical insight into how host and viral factors contribute to disease severity.

Neutrophils have an inherent capacity of recognizing infectious agents, in addition to acting as sites of infection, in both cases resulting in an acute inflammatory response (Galani and Andreakos, 2015). Understanding the precise nature of the inflammatory response and the pathophysiological consequences, could identify pathways for therapeutic intervention based on early detection of a prognostic signature for COVID-19 outcomes. An uncontrolled, hyper-inflammatory response, known as a “cytokine storm” can result from a massive influx of innate leukocytes, inclusive of neutrophils and monocytes (Bordon et al., 2013), and has been heavily implicated in patients with severe COVID-19 (Borges et al., 2020; Huang et al., 2020a). Cytokine storm and presence of pro-inflammatory mediators can be a predictor of disease severity and often leads to acute respiratory distress syndrome (ARDS), and eventually respiratory failure (Fajgenbaum and June, 2020). Retrospective studies have also demonstrated that elevated levels of interleukin-6 (IL-6) are a strong predictor of mortality over resolution (Ruan et al., 2020), and tumor necrosis factor alpha (TNFα) is increased in severe compared to moderate cases (Chen et al., 2020).

Despite their importance in anti-viral immunity and response to viral pathogens, neutrophils have been somewhat overlooked for their role in the pathogenesis of SARS-CoV-2 infection (Hemmat et al., 2020; Shi et al., 2020; Veras et al., 2020a). It has been shown that the number of neutrophils in the lower respiratory tract correlates to disease severity in other viral infections, including influenza A infection (Radermecker et al., 2019) and, more recently, to also be a feature of COVID-19 pathology (Veras et al., 2020a). Several studies have highlighted the importance of neutrophils in the response to SARS-CoV-2 infection (Li et al., 2020; Shi et al., 2020; Tomar et al., 2020; Veras et al., 2020a) and clinically neutrophil-lymphocyte ratios (NLR) are becoming an important hallmark of severe COVID-19 (Qin et al., 2020). Furthermore, the expression of angiotensin converting enzyme 2 (ACE2) on neutrophils has also been demonstrated; (Arcanjo et al., 2020; Janiuk et al., 2021; Veras et al., 2020b)(Veras et al., 2020c). These studies, however, have primarily focused on the production of neutrophil extracellular traps and lack insights into other neutrophil functional responses such as inflammatory cytokine production and viral internalization in neutrophils.

Studies in animal models, such as hamsters and ferrets, show that the development of a robust immune response soon after viral exposure is able to rapidly clear infection, with viral DNA only being detected in the airways of hamsters (Monchatre-Leroy et al., 2020). Inflammatory cell infiltrates correlated with high presence of SARS-CoV-2 viral RNA detected in upper airway epithelium of the hamsters (Monchatre-Leroy et al., 2020). Similarly, high numbers of neutrophils were detected in luminal upper airways associated with bronchiolitis in inoculated ferrets (Monchatre-Leroy et al., 2021; Ryan et al., 2021). Although this provides valuable information regarding SARS-CoV-2 infection, animal models have not yet been observed to develop severe COVID-19-related pathologies as seen in humans, demonstrating the importance of investigations in human based tissue and cellular models.

In this study, the relationship between SARS-CoV-2 infection and pre-existing airway neutrophilia in the presence of the lung airway epithelial niche was evaluated through the development of a co-culture infection model. Primary neutrophils were isolated from peripheral blood and co-cultured with differentiated primary tracheo-bronchial airway epithelium prior to infection with live SARS-CoV-2 virus. Changes in the inflammatory profile and epithelial response were comprehensively evaluated to determine the impact of neutrophils on the epithelial SARS-CoV-2 infection.

Methods

Isolation of neutrophils from peripheral blood

Neutrophils were isolated from fresh human peripheral blood with patient consent and approval of the Institutional Review Board (IRB) of the University of Southern California (USC), protocol #HS-20-00546. CD15-expressing neutrophils were isolated using the EasySep™ direct neutrophil isolation kit (Stem Cell Technologies, Seattle, WA) within 1 hour of the blood draw as per the manufacturer's instructions. Briefly, 5 ml of peripheral blood was collected into 10 ml EDTA vacutainers (Becton Dickinson, Franklin Lakes, NJ). From this, 3 ml was diluted 1:1 with PBS (Thermo Fisher Scientific, Waltham, MA) and kept on ice for purity analysis by flow cytometry. The remaining 2 ml was transferred to a 5 ml polystyrene round bottomed tube (Genesee Scientific, San Diego, CA) and gently combined with 100 µl of isolation cocktail and 100 µl of RapidSpheres™ (Stem Cell Technologies). After incubation at room temperature for 5 mins, 1.8 ml of 1 mM EDTA was added, gently mixed, and placed into the EasySep™ Magnet (Stem Cell Technologies) for 5 mins. The enriched cell suspension was placed into the EasySep™ Magnet for an additional 5 mins and decanted into a fresh tube. Approximately 4.25 x 10^6 cells were isolated from 5 ml of peripheral blood.

Flow activated cell sorting (FACS)

To validate the purity of neutrophils isolated from peripheral blood; 1x10^7 $CD15^+$ freshly isolated human neutrophils were resuspended in 100 ul FACS buffer (PBS, 0.5mM EDTA, 1% FBS, 0.1% BSA) and fresh whole human blood diluted 1:5 in FACS buffer and supplemented with 5 ul of human TruStain Fc receptor blocker (Biolegend, San Diego, CA) for 5 mins on ice. Cells were then incubated with anti-human CD15 PE (Biolegend) for 1 hour prior to FACS analysis. Cells were analyzed on the Sorp FACS Symphony cell sorter (BD Biosciences) in the Flow Cytometry Core facility at USC using FACS Diva software and all analyses was carried out in Flow Jo V10.8.0 (BD Biosciences).

Air-liquid interface (ALI) differentiation of airway epithelium

Primary human airway basal epithelial cells (HBEC) were isolated from explant human lung tissue as previously described (Randell et al., 2001) and with approval of the IRB at the University of Southern California (USC) (protocol #HS-18-00273). For this study, HBEC donors were randomly paired with blood neutrophil donors. HBECs were expanded for 1 to 4 passages in airway epithelial cell growth media (AEGM, Promocell,

Heidelberg, DE) and transitioned to Pneumacult Ex+ (Stem Cell Technologies) for 1 passage, prior to growth on Transwells. Cells were routinely passaged at 80% confluence using Accutase™ (Stem Cell Technologies) and seeded at 5 x 10^4 cells per 6.5 mm polyethylene (PET) insert with 0.4 µm pores (Corning, Corning, NY). Media was changed every 24-48 hours and transepithelial electrical resistance (TEER) was monitored every 24-48 hours using an EVOM3 epithelial volt-ohm meter (World Precision Instruments, Sarasota, FL). At resistances ≥ 450Ω ^cm^2, cells were air lifted by removing the apical media and washing the apical surface with phosphate buffered saine (PBS, Sigma-Aldrich, St Louis, MO). The basolateral media was replaced with Pneumacult ALI media (Stem Cell Technologies) and changed every 2 to 3 days for up to 40 days.

For differentiated spheroids, transwells were pre-treated with 25% (v/v) of Matrigel in Pneumacult Ex+ (Stem Cell Technologies) for at least 1 hour at 37°C. For spheroid formation, a single cell suspension of HBECs was generated using with Accutase. Single cells were resuspended in Matrigel™ 5% in Pneumacult Ex+. The cell suspension was loaded onto the pre-established gel-bed and Pneumacult Ex+ media added to the lower chamber. After 3 days the media was exchanged for Pneumacult ALI maintenance media (Stem Cell Technologies) and changed every 2~3 days.

SARS-CoV-2 culture

Vero E6 cells overexpressing ACE2 (VeroE6-hACE2) were obtained from Dr. Jae Jung and maintained in DMEM high glucose (Thermo Fisher Scientific, Waltham, MA), supplemented with 10% FBS (Thermo Fisher Scientific, Waltham, MA), 2.5 ug/ml puromycin (Thermo Fisher Scientific, Waltham, MA) at 37˚C, 5% CO_2 in a humidified atmosphere in the Hastings Foundation and The Wright Foundation Laboratories BSL3 facility at USC. SARS-CoV-2 virus (BEI resources, Manassas, VA) was cultured and passaged 4 times in VeroE6-hACE2 cells and harvested every 48 hours post-inoculation. Plaque forming units (PFU) were determined using a plaque assay by infecting a monolayer of VeroE6-hACE2 cells with serial dilutions of virus stocks and layering semi-solid agar. Plaques were counted at day 3 post infection to determine PFU. Virus stocks were stored at -80˚C.

SARS-CoV-2 infection

Differentiated airway epithelium at ALI was cultured with addition of 50 µl of PBS to the apical surface and incubated at 37°C, 5% CO_2 in a humidified atmosphere. After 10 minutes PBS was removed to eliminate the

mucus build-up on the apical surface. The basolateral culture media was removed and replaced with 400 µl of assay media (Bronchial Epithelial Growth Media (BEGM), Lonza, Walkersville, MA), without the addition of bovine pituitary extract, hydrocortisone & GA-1000, for 1 hour prior to the addition of neutrophils. Freshly isolated neutrophils were diluted to 5 x10^6 cells/ml in Hank's Balanced Salt Solution (with $Mg2^+$ and $Ca2^+$) (Thermo Fisher Scientific, Waltham, MA) and 20 µl of this suspension was seeded onto the apical surface of the ALI cultures. Monocultures of airway epithelium and neutrophils were used as controls. The neutrophil-epithelial co-cultures were incubated for 1 hour during which they were transferred to the BSL3 facility for infection. Co-cultures were infected with 1x10^4 PFU of SARS-CoV-2 in 100 µl of OptiMEM (Thermo Fisher Scientific, Waltham, MA) added to the apical surface. Infected cell cultures were incubated for 4 hours at 37°C, 5% CO_2 in a humidified atmosphere. After infection, the apical and basolateral supernatants were collected, and SARS-CoV-2 was inactivated with 1% Triton-X (Sigma-Aldrich, Burlington, MA) in PBS for 1 hour. Culture supernatants were stored at -20ºC until required.

Validation of virus inactivation

SARS-CoV-2 virus was inactivated by addition of 10% Triton-X to supernatants to generate a final concentration of Triton-X of 1% and incubating at room temperature for 1 hour. PFU was quantified using a plaque forming assay with ACE2 over-expressing Vero E6 cells (VeroE6-hACE2). Serial dilutions of SARS-CoV-2 virus were performed from a stock concentration of 1x10^5 PFU/ml and inactivated with 1% Triton-X at room temperature for 1 hour and used to infect Vero E6 cells for a total of 4 days. Cells were monitored routinely for cytopathic effects using the Revolve microscope (Echo Laboratories, San Diego, CA).

RNA isolation and qRT-PCR

RNA was collected in 100 µl of Trizol (Thermo Fisher Scientific, Waltham, MA) per insert and incubated for 15 mins at room temperature. Cell isolates were gently mixed by pipetting up and down. An additional 900 µl of Trizol was added and cell isolates were collected and stored at -80°C until required. Cellular RNA was isolated by either phenol/chloroform extraction or using the Direct-zol RNA Microprep kit (Zymo Research, Irvine, CA). RT-qPCR was performed in 384 well plates on an Applied Biosystems 7900HT Fast Real-Time PCR system using the QuantiTect Virus Kit (Qiagen, Redwood City, CA) and SARS-CoV-CDC RUO primers and probes (Integrated DNA Technologies (IDT), Coralville, IA). Briefly, each 5 µl reaction contained 1 µl 5x

QuantiTect Virus Master Mix, 500 nM forward primer, 500 nM Reverse Primer, 125 nM Probe, 10 ng DNA, 0.05 µl QuantiTect Virus RT Mix, and DNAse/RNAse-free water up to a final volume of 5 µl. Calibration curves for RNAseP primers/probe was performed with 10-fold dilutions of RNA from uninfected Calu3 cells (ATCC, Manassas, VA) from 100 ng to 0.01 ng per reaction. Calibration curves for N1 primers were performed on 5 ng of RNA from uninfected Calu3 cells per reaction spiked with 10-fold dilutions from 50 ng to 0.005 ng of RNA from Calu3 cells collected 48 hours post infection. Relative gene expression was calculated using the Pfaffl method (Pfaffl, 2001).

Immunohisto-/cyto-chemistry

Primary human lung tissue from post-mortem or surgical resection donors (detailed in Supplemental **Table S1**) was fixed in 10% neutral buffered Formalin (Thermo Fisher Scientific, Waltham, MA). The tissue was then dehydrated in 70% ethanol (Thermo Fisher Scientific, Waltham, MA) prior to embedding in paraffin blocks for sectioning. Tissue sections were mounted on positively charged slides (VWR, Visalia, CA) and tissue was rehydrated through sequentially decreasing concentrations of ethanol (100% - 70%) and finally water. Slides were stained sequentially with Hematoxylin and then Eosin and imaged on the Olympus microscope IX83 (Olympus, Waltham, MA). Alternatively, tissue slides were incubated overnight at 60°C in Tris-based antigen unmasking solution (Vector Laboratories, Burlingame, CA) before permeabilization in 3% BSA, 0.3% Triton-X 100 in PBS for 1 hour and blocking in 5% normal donkey serum (Jackson ImmumoResearch, West Grove, PA) for 1 hour at room temperature. *In vitro* co-cultures were fixed in 4% PFA (Thermo Fisher Scientific, Waltham, MA) for 1 hour at room temperature and stored in PBS at 4ºC to be used for immunohisto/cytochemistry. Co-cultures were then permeabilized and blocked in 3% BSA, 0.3% Triton-X 100 in PBS for 1 hour and blocking in 5% normal donkey serum (Jackson ImmumoResearch, #017-000-121) for 1 hour at room temperature. Tissue sections and *in vitro* cultures were subsequently stained with the antibodies or RNAScope probes listed in **Supplemental Table S1**. Slides were mounted in Fluoromount-G (Thermo Fisher Scientific, Waltham, MA) and imaged on a DMi8 fluorescent microscope (Leica, Buffalo Grove, IL) or a Zeiss LSM 800 confocal microscope (Zeiss, Dublin, CA).

Spheroids were fixed with 4% PFA in PBS at 5, 10, 14 and 20 days after the culture. For immunostaining, spheroids, attached at the bottom of the transwells, were pre-treated with 0.1% of Triton X-100 in PBS (hereinafter 0.1% PBT) for 10 min for permeabilization. The cells were incubated with primary antibody for

1hr 30min at room temperature and washed with 0.1% PBT. Secondary antibodies were incubated for 45 min at room temperature and washed with 0.1% PBT. Nuclei were stained with DAPI. The spheroids were mounted with Fluoromount G (#0100-01; SouthernBiotech). The spheroid images were taken with confocal microscope (Zeiss, LSM710) using a Plan Apochromat 63x/1.4 NA oil-immersion objective, ~10 μm of thickness with 0.4μm of z-stack interval and processed with ZEN software (Zeiss) and ImageJ software.

Single Cell RNA sequencing and Bioinformatic Analysis

Gene expression counts (GEO accession number: GSE150674, (Carraro et al., 2021)) from both the fresh isolates and ALI cultures were processed using functions in the R package Seurat (version 4.0.2) (1). For each sample, low quality cells and potential cell doublets were removed by filtering cells based on the number of genes detected and the fraction of reads mapping to the mitochondrial genome. Cells with less than 200 genes detected or greater than 4,900 – 7,000 genes detected (depending on the sample) were removed as well as cells with greater than 10% of mitochondrial reads. The filtered gene counts were then integrated into a unified data set using the SCTransform (2) based integration workflow implemented in Seurat. The first 30 PCs were used as the number of dimensions for the FindNeighbors and FindClusters functions. To find the optimal clustering resolution value we explored a range of resolution values from 0 to 2 by increments of 0.2. We then visualized the range of cluster resolutions using the R package clustree (version 0.4.3) (3). A final resolution of 0.4 was selected and used for downstream analyses. Clusters were visualized in two-dimensional space using the RunUMAP function in Seurat. Cluster specific cell types were annotated manually by examining the expression of canonical marker genes within a given cluster and clusters with shared marker gene expression patterns were collapsed. The fresh isolates and ALI couture data sets were analyzed separately.

Transepithelial Electrical Resistance

Pre-warmed Assay media (200 µl) was added to the apical surface of the cultures and TEER was measured using an EVOM-3 meter (World Precision Instruments, Sarasota, FL).

Meso Scale Discovery cytokine assay

50 µl of apical and 50 µl basolateral cell culture supernatants were analyzed for cytokines using the Meso Scale Discovery (MSD) V-plex Viral Panel 1 Human Kit (Meso Scale Diagnostics, Rockville, MA) as per the manufacturer's instructions. Briefly, 1:5 dilutions of cell supernatant samples were diluted in PBS containing 1% Triton-X. Samples were added to the MSD plate along with a 7-point 4-fold serial dilution (from 10,000 pg/ml to 0.6104 pg/ml) of protein standards diluted in PBS with 1% Triton-X. The MSD plate was sealed, and samples incubated at room temperature for 2 hours. The plate was washed 3x in wash buffer and 25 µl of secondary antibody was added to each well. Plates were sealed and incubated at room temperature for a further 2 hours in the dark. Plates were washed 3x with wash buffer and 50 µl of 2x read buffer (MSD R92TC) was added to each well. The plates were read on the MESO Sector S 600 (Meso Scale Diagnostics) and concentrations determined against the standard curve.

Viral Internalization Assay

CD15+ neutrophils were seeded at 20,000 cells per well in in HBSS with or without 15 µM Cytochalasin D (Sigma Aldrich, Burlington) black walled 96 well plates (Thermo Fisher Scientific, Waltham, MA) for 1 hour to allow for attachment. Cells were then infected with SARS-CoV-2 at 2 MOI (80 µl at 5x10^5 PFU/ml) for 4 hours. Cells were then washed 2 x with PBS and fixed in 4% PFA. Cells were stained for SARS-CoV-2 RNA via RNAScope and DAPI as per the manufacturer's instructions. Whole wells were supplemented with 50 µl of PBS post staining and well were scanned on the DMi8 fluorescent microscope (Leica, Buffalo Grove, IL)). Total cell number was determined by total frequency of DAPI particles and infected cells determined by SARS-CoV-2 particle signal in proximity to DAPI. Images were analyzed with ImageJ software 1.52n (National Institute of Health, Bethesda, MA).

Data Analysis and Statistics

All data are presented as mean ± S.E.M. Statistical analysis is dependent upon the data set and is specifically indicated in each figure. For comparisons of 2 groups. a two-tailed unpaired Student's T-test was used. For more than 2 groups, an analysis of variance (ANOVA) was used with a post hoc Tukey test. Significance is determined to be $P<0.05$. All data represents a minimum of three independent biological replicates (N=3), each with 3 experimental replicates (n=3). Data was presented and analyzed using Graph Pad prism v8.4.3 (GraphPad, San Diego, CA).

Results

Airway epithelial pathologies are associated with neutrophil activity in severe COVID-19.

To evaluate lung pathologies associated with severe COVID-19 patients, we obtained formalin-fixed paraffin embedded (FFPE) tissue sections from two post-mortem COVID-19 patients, kindly provided by autopsy service at the University of Vermont Medical Center (UVMMC). Hematoxylin and Eosin (H&E) stained tissue sections were analyzed, and pathologies determined by an independent pathologist to be consistent with severe ARDS with mixed inflammatory cell infiltrates, inclusive of neutrophils, and organizing pneumonia (**Fig. 1A-D**). Tissues from patient Au20-39 (detailed in **Supplemental Table S1**) contained a mild infiltrate of chronic inflammatory cells surrounding the bronchiole and arterial tissues with involvement in the adjacent surrounding alveolar tissue (**Fig. 1A** and **Supplemental Fig. S1A**). Scattered giant cells were identified in alveolar spaces and within the interstitium (**Fig. 1B,** indicated by the red arrows and **Supplemental Fig. S1B**). No well-formed granulomas or definite viral inclusions were evident in this patient. Images from the second patient; Au20-48 **(**detailed in **Table S1)** also show severe organizing diffuse alveolar damage with evidence of barotrauma (**Fig. 1C** and **Supplemental Fig. S1D**). Alveolar spaces are lined by hyaline membranes or filled with polyps of organizing pneumonia and chronic inflammation (**Supplemental Fig. S1D**). Alveolar walls are expanded with edema and a mixed inflammatory cell infiltrate including neutrophils (**Supplemental Fig. S1C-D**). Bronchioles demonstrate chronic injury with peribronchiolar metaplasia and early squamous metaplasia (**Fig. 1D** and **Supplemental Fig. S1C**). Organizing pulmonary emboli are present in several arteries (**Supplemental Fig. S1C-D**). There are frequent rounded airspaces lined by inflammatory cells and giant cells, consistent with barotrauma from ventilation injury (**Supplemental Fig. S1D**). There are also scattered giant cells in the interstitium not associated with the barotrauma (**Supplemental Fig. S1C-D**).

Given the extensive infiltration of inflammatory cells, inclusive of neutrophils, we further evaluated the neutrophil-related tissue pathology in both patients. An array of airway tissue pathologies were evident in both tissues including 1) basal cell hyperplasia and small airway occlusion (**Fig. 1A-E**) 2) epithelial damage and tissue remodeling of smaller ciliated airways (**Fig. 1F**) 3) epithelial shedding of large cartilaginous airways (**Fig. 1G**), 4) neutrophil invasion into the airway lumen (**Fig.1H**), and finally, 5) neutrophil invasion in the alveolar space with associated alveolar tissue damage and remodeling (**Fig. 1I**).

In each of these examples found in post-mortem COVID-19 tissue, neutrophils were detected and frequently demonstrated increased neutrophil elastase (NE) activity, compared to neutrophils detected in tissue from no underlying respiratory disease. Interestingly, we noted that neutrophils strongly expressed ACE2 in these tissues. We confirmed ACE2 expression in neutrophils present in human lung tissues by immunofluorescence, comparing tissue from patients with no underlying respiratory disease and patients with CF (**Supplemental Fig. S2A-B**), a chronic lung disease where neutrophilia is a common hallmark. In these tissues, ACE2 expression was confirmed to co-localize with both NE and CD15 (**Supplemental Fig. S2C-D)**. We further validated ACE2 expression in CD15+ purified neutrophils from peripheral human blood, purity of neutrophils was confirmed by FACS (>97%) (**Supplemental Fig. S2E).**

Polarized inflammatory responses to SARS-CoV-2 are detected in an *in vitro* model of neutrophilic airways.

Given the prevalence of neutrophilia in the airways of patients with chronic airway disease (Jasper et al., 2019) and its association with other SARS-CoV-2 co-morbidities, such as diabetes mellitus (Thomson et al., 1997) and hypertension (Florentin et al., 2021; Taylor et al., 2018), we proceeded to investigate the impact of neutrophilic airway inflammation in SARS-CoV-2 infection. We created a neutrophilic airway *in vitro* model by co-culturing $CD15^{+}$ peripheral blood polymorphonuclear leukocytes (PMNs) with primary human tracheo-bronchial airway epithelial cells (HBECs) differentiated at the air-liquid interface (ALI), and infected these cultures with live SARS-CoV-2 virus for 4 hours (**Fig. 2A**). This 4-hour time point allows us to profile the acute phase cellular viral response, i.e., degranulation of the neutrophils. The short time frame for analysis was chosen to both eliminate significant viral replication and thus anticipate any detectible viral load is as a result of initial infection (Zhu et al., 2020b), and to allow for optimal investigation into neutrophil function without loss of viability interfering with the assays due to the relatively short half-life of neutrophils. Prior to infection we confirmed the expression of ACE2 and Transmembrane Serine Protease 2 (TMPRSS2 in our *in vitro* airway epithelium models (**Supplemental Fig. S3)**. While ACE2 RNA was relatively low in expression across basal, secretory and multiciliated cells (**Supplemental Fig. S3B-C**) at the protein level a predominant colocalization was detected with multiciliated cells in the airways (**Supplemental Information and Fig. S3A, D-F)).** This data supported by similar analysis of human lung tissues (**Supplemental Fig. S4**) where we observed a

similarly low level of expression in RNA in basal, secretory and multiciliated cells (**Supplemental Fig S4A-B**) while protein, detected by IF, was associated with multiciliated cells and cells in submucosal gland (**Supplemental Fig S4C-F**). Confirmation of ACE2 expression at the RNA and protein level in human lung tissues and our *in vitro* model supports currently published data evaluating ACE2 in human lung tissue (Jia et al., 2005; Jia et al., 2009; Zhang et al., 2020b).

SARS-CoV-2 viral RNA was detected in the co-cultures using RNAscope (**Fig. 2B**) confirming infection of the airway epithelium. Interestingly, NE activity was heavily centered around sites of SARS-CoV-2 infection and internalization of SARS-CoV-2 by neutrophils was confirmed by co-localization of staining for NE and SARS-CoV-2 viral RNA (**Fig. 2B**, indicated by the orange arrows). In our model system the apical side of the epithelium comprises predominantly multiciliated and secretory cells directly exposed to neutrophils and the virus, the basolateral side contains predominantly basal cells. To further understand whether a polarized inflammatory response exists in response to SARS-CoV-2 infection we evaluated the apical and basolateral compartments independently. Apical and basolateral cell culture supernatants were analyzed for secretion of inflammatory cytokines using the meso scale discovery (MSD) cytokine assay. As shown in **Figure 2C-D** a differential inflammatory profile exists between the apical and basolateral compartments. Surprisingly, in the absence of neutrophils, there was no significant difference in cytokine release from the airway epithelial cells upon SARS-CoV-2 infection, except for basolateral interleukin-8 (IL-8) which significantly increased from 6180 ±1751 to 52996±17121 pg/ml, $p<0.05$). As IL-8 is a major chemoattractant for neutrophils this suggests that the basolateral surface responds to viral infection with a predominant release of IL-8, likely in the attempt to recruit neutrophils to the epithelium (Baggiolini et al., 1989; Parsons et al., 1985; Yoshimura et al., 1987). The addition of neutrophils to differentiated airway epithelium, creating a neutrophil-epithelial co-culture in the absence of any infection, resulted in a significant increase in the secretion of interferon gamma (IFNγ, 634±1.6%, $p<0.01$) and IL-10 (273±11.6%, $p<0.01$) at the apical surface with notable, but not statistically significant increases also in TNFα (**Fig. 2C**). At the basolateral surface the presence of neutrophils also stimulated the release of IFNγ (321±4.1%, $p< 0.05$) and IL-10 (341±8.5%, $p<0.01$) and additionally significantly increased the release of IL1-β (557±4%, $p<0.0001$) and IL-4 (220±3%, $p<0.001$) (**Fig. 2D**). This data suggests that the presence of neutrophils at apical surface and infiltrating the airway epithelium stimulates the release of pro-inflammatory cytokines from both the apical and basolateral faces of the

epithelium, thus creating a pro-inflammatory niche in the co-cultures. In our model, this pro-inflammatory niche was used to recreate aspects of chronic airway inflammation in the human lung. Interestingly, the presence of neutrophils did not stimulate significant changes in IL-8 secretion from the basolateral surface supporting the role for IL-8 in the recruitment phase of airway neutrophilia which is already achieved in our model (Azevedo et al., 2021; Pease and Sabroe, 2002).

In parallel, we infected these neutrophilic airway models with live SARS-CoV-2 virus and compared directly to both the infection in the absence of neutrophils and the neutrophilic airway in the absence of infection. The changes in the inflammatory cytokine release from both the apical and basolateral surfaces was significantly higher than either the infection only or neutrophil only co-cultures, indicating that there is a significant cross talk between neutrophils and the airway epithelium altering the inflammatory response (**Fig. 2C-D**). Compared to the infection only cultures, infection of the co-culture resulted in a significant increase in the apical secretion of IFNγ, IL1-β, IL-6 and IL10 (1030±5%, $p<0.0001$, 169±6%, $p<0.05$, 580±8% $p<0.0001$ and 231±3%, $p<0.001$. respectively) (**Fig. 2C**) and in the basolateral secretion of IFNγ, IL1-β, IL-4, IL-6, IL10 and TNFα (261±5%, $p<0.05$, 572±6% $p<0.0001$, 203±5% $p<0.001$, 593±8% $p<0.0001$, 279±8% $p<0.001$ and 316±2%, $p<0.001$ respectively) (**Fig. 2D**). Compared to the uninfected neutrophil co-cultures, co-culture infection resulted in a significant increase in the apical secretion of IFNγ, IL1-β, IL-4, IL-6 and IL10 (338±5%, $p<0.0001$, 161±6%, $p<0.05$, 221±18% $p<0.05$, 593±7% $p<0.0001$ and 136±3%, $p<0.05$, respectively) and in the basolateral secretion of IL10 and TNFα (156±8%, $p<0.001$ and 167±3%, $p<0.01$ respectively) (**Fig. 2C**). The only instance where TNFα was significantly changed apically was in the infected co-cultures relative to uninfected epithelial cell monocultures with a 329±13%, $p<0.05$ increase. This data indicates a significant augmentation of the inflammatory response when infection occurs in the presence of pre-existing airway neutrophilia. Importantly, this secretion profile closely reflects the cytokine biomarkers that have been clinically identified in patients hospitalized with severe COVID-19 disease (Del Valle et al., 2020; Han et al., 2020; Liu et al., 2020b), highlighting the importance of the co-culture models in recapitulating features associated with more severe responses to SARS-CoV-2.

Increased in viral load of SARS-CoV-2 in epithelial cells is associated with disruption in epithelial barrier integrity.

Inflammation is known to breakdown tight junction barriers, such as that of the respiratory epithelium. To determine whether the presence of a proinflammatory niche (i.e., in the case of pre-existing neutrophilia) impacts epithelial barrier integrity and viral load of the epithelial cells we evaluated barrier resistance and viral content of the airway epithelium. Trans epithelial electrical resistance (TEER) was recorded at 4 and 24 hours after introduction of neutrophils to the airway epithelium. The presence of neutrophils significantly reduced TEER and, therefore, epithelial barrier integrity, by 23±9%, $p<0.05$ after 4 hours. This reduction in TEER was sustained through 24 hours (22±4%, $p<0.05$), all data are compared to epithelial monocultures (**Fig. 3A**). Evaluation of viral load by qRT-PCR for SARS-CoV-2 nucleocapsid RNA in the epithelial cells under the same conditions indicated a concurrent and significant increase in infection after the addition of neutrophils by 3.1±1.1-fold ($p<0.05$) (**Fig. 3B**). In the absence of infection, no SARS-CoV-2 RNA was detected (data not shown). To determine whether the pro-inflammatory cytokines released in response to SARS-CoV-2 based on the data in **Fig. 2** and known to be secreted by neutrophils, could induce similar changes in epithelial barrier function we supplemented the culture media with IFNγ (10 ng/ml), IL-1β (10 ng/ml), IL-6 (10 ng/ml) and TNFα (10 ng/ml) (referred to as cytomix). In the presence of cytomix without neutrophils a similar decline in TEER after 4 hours (18±7%, not significant) was observed, further declining to 30±5%, $p<0.05$ after 24 hours (**Fig. 3C**). This similarly corresponded to an increase in viral infection of the airway epithelium (2.6±0.5-fold, $p<0.05$) in the presence of cytomix (**Fig. 3D**). This indicates that in epithelium where chronic neutrophil infiltration is present there is a significant deterioration in epithelial barrier function which is associated with elevated cytokine levels and an increase in viral infection of the epithelium.

Phagocytosis of SARS-CoV-2 is the predominant mechanism of viral internalization in neutrophils.

Finally, to determine whether the expression of ACE2 protein in neutrophils has a significant impact in the response of neutrophils to SARS-CoV-2, we evaluated whether neutrophils were being actively infected via a physical interaction of ACE2 and SARS-CoV-2 or phagocytosing the SARS-CoV-2 virus. To better understand this, the frequency of SARS-CoV-2 internalization in monocultures of neutrophils was quantified in the presence or absence of cytochalasin D (15 μM) to inhibit phagocytosis (**Fig. 4A**). The number of neutrophils positive for SARS-CoV-2 RNA, reflecting viral internalization, relative to the total number of neutrophils was calculated after infection of the cells with SARS-CoV-2 (MOI = 2). Infection, detected by RNA scope, occurred at a rate of 7.9±1% of neutrophils in culture. This signal was significantly reduced by from

7.9±1% to 1.3±0.3% in the presence of cytochalasin D (**Fig. 4B**). Disruption of the actin cytoskeleton, a core component of phagocytosis, therefore, significantly reduced viral uptake in neutrophils. This suggests the primary mechanism for SARS-CoV-2 internalization in neutrophils is phagocytosis.

Discussion

It is well established that neutrophils are critical in the development of pathological inflammation which can result in both acute and chronic tissue damage. Upon evaluation of post-mortem COVID-19 tissues we observed significant neutrophil presence and activation in regions closely associated with pathogenic alterations in the airway epithelium. In addition, we know that many associated co-morbidities, including chronic airway disease (Gernez et al., 2010; Jasper et al., 2019), aging (Chen et al., 2014; Kulkarni et al., 2019; Sapey et al., 2017) and obesity (Kordonowy et al., 2012; Maia et al., 2019; Manicone et al., 2016) are also associated with chronic airway inflammation. In this study we, therefore, developed a model to evaluate neutrophil-epithelial interactions and how this may be critical in the progression to severe COVID-19. Using this model, we were able to conclude that the presence of neutrophils with the airway epithelium significantly augments the proinflammatory responses to SARS-CoV-2, increases airway viral load and decreases airway epithelial barrier integrity. Our data, therefore, supports a key role for neutrophil-epithelial interactions in determining the infectivity and outcome measures of COVID-19.

Using primary human cells in a co-culture of epithelial and inflammatory cells overcomes some of the limitations of more widely used model systems to study SARS-CoV-2 infection. Although considered the gold standard providing the opportunity to study infection *in vivo*, the relevance of animal models in mimicking human lung pathophysiology is unclear, particularly with respect to SARS-COV-2. To date, although infection can be detected, no animal model had closely reflected COVID-19 pathogenesis that leads to severe symptoms and fatal lung disease (Kumar et al., 2020; Munoz-Fontela et al., 2020). Furthermore, studying neutrophilia in animal models is challenging, several depleted or knockout models exist (Stackowicz et al., 2019), however evaluation of elevated lung neutrophilia typically requires pro-inflammatory stimulation with lipopolysaccharide (LPS) (Corteling et al., 2002), this could complicate interpretation of findings in relation to viral infection. Many studies investigating the cellular and molecular mechanisms of SARS-CoV-2 infection have used studied in cell lines, such as HELA, or HEK cells, which themselves lack expression of ACE2. This limitation is overcome by overexpressing human ACE2, or by using airway epithelial cell lines, such as A549 or CALU3 cells, which are derived from lung cancers and, while epithelial in origin, are limited in their capacity to represent the biology and physiology of a normal differentiated human airway epithelium. In our study, using primary human airway epithelial cells, we have a model that investigates infection of some of the first

cells in the human body exposed to the virus that express endogenous levels of ACE2 and TMPRSS2. After characterization of expression of ACE2 throughout the proximal airway epithelium (**Supplemental Fig S4**) and in our *in vitro* model system (**Supplemental Fig. S3**) we observe a similar distribution of ACE2. Both transcript and protein levels are relatively low in the proximal airway epithelium with the highest expression associated with multiciliated cells and SMG cells, supporting the observations of others (Jia et al., 2005; Jia et al., 2009; Zhang et al., 2020b). To best capture mechanisms relevant to *in vivo* human SARS-CoV-2 infection it is important that an *in vitro* co-culture model can mimic the pro-inflammatory cytokine biomarker observations that are documented clinically or observed in intact SARS-CoV-2 infected human tissues from patients developing severe COVID-19 disease. In tissues from severe COVID-19 patients we observed a significant presence of neutrophils and neutrophil activity in and surrounding patient airways, including neutrophil invasion into the airway lumen, epithelial shedding, and large amounts of NE activity (**Fig. 1** and **Supplemental Fig. S1-2**). Highlighting a key role for neutrophils in the response to SARS-CoV-2 infection. Our model is designed to mimic neutrophilic airway inflammation associated with chronic lung disease, that has been linked with a predisposition to developing more severe COVID-19 disease.

It is established that neutrophil phenotype and function, including those involved in resolving viral infections, is strongly regulated by signals received from their tissue micro-environment (Parkos, 2016), in our study we considered neutrophil responses in the presence of an epithelial micro-environment, a major advantage of our model for studying SARS-CoV-2 infection. Through paired comparisons to primary airway epithelial cells in monoculture, we were able to demonstrate key differences in the secretion of pro (IFNγ, IL1β, IL-6, IL-8 and TNFα) and anti-inflammatory (IL-4 and IL10) mediators, epithelial barrier integrity and infectivity of epithelial cells (**Fig. 2**), which would have been over-looked in monoculture experiments involving airway infection only. Importantly, the secretion of pro-inflammatory cytokines in our model is consistent with clinical studies that have reported an elevated inflammatory profile associated with severe COVID-19 disease. In patient peripheral blood samples, IL-6 (Godkin and Humphreys, 2020; Huang et al., 2020b; Liu et al., 2020a; Yang et al., 2020) IL-10 (Godkin and Humphreys, 2020; Liu et al., 2020a) are consistently higher in COVID-19 patients and correlate with disease severity. Additionally, IL-6 and IL-8 are even higher in ICU than the IMU (Pandolfi et al., 2020). Our data also closely mimics responses observed in primate models of the disease (Fahlberg et al., 2020). Furthermore, the correlation of neutrophilic recruitment to the airways is also clinically

relevant where substantially elevated neutrophil are observed in the peripheral blood of COVID-19 patients and neutrophil-to-lymphocyte ratios correlate with severe and fatal complications related to ARDS (Godkin and Humphreys, 2020; Huang et al., 2020b; Qun et al., 2020; Zhu et al., 2020a). Additionally, marked increases in neutrophils were also observed in bronchiolar alveolar lavage (BAL) fluids from patients admitted into the intensive care unit (ICU) compared to intermediary medical unit (IMU) patients correlating to disease severity (Pandolfi et al., 2020). The lack of robust inflammatory response of the epithelium alone may also provide rational for why some people are predisposed to more severe responses than others. In fact, our data evaluating the response of the more proximal, cartilaginous airways may highlight the importance of a robust proximal airway defense mechanism that controls the progression to severe COVID-19 associated with ARDS and distal airway dysfunction. The distinct polarized secretion of IL-8 in response to SARS-CoV-2 infection in the monocultured epithelial cells, indicates a signaling from the epithelium to recruit neutrophils, IL-8 is the core chemoattractant for neutrophils (Baggiolini et al., 1989; Kunkel et al., 1991; Parsons et al., 1985; Yoshimura et al., 1987). This response was not observed in the neutrophil-epithelial co-cultures and suggests that the epithelial cells can recognize neutrophils within their microenvironment.

Pro-inflammatory cytokines, including IFNγ, IL1β, IL-6 and TNFα, have extensively been shown to disrupt barrier integrity and permeability of the epithelium (Al-Sadi et al., 2009; Capaldo and Nusrat, 2009). This breakdown in barrier integrity exists to allow for leukocyte migration to sites of stress and infection. Theoretically, any tight-junction breakdown that allows for more leukocyte migration, would also allow for increased permeability for viral particles to sub-apical and sub-epithelial structures, thus increasing infectivity and cellular viral loads. In our data we show that neutrophils and cytomix both synonymously decrease barrier integrity (**Fig. 3).** This association of epithelial barrier integrity with an increase in viral load suggests that, at least in part, the epithelial barrier integrity plays an important functional role in resisting SARS-CoV-2 infection.

Finally, we addressed the key question of whether neutrophils are actively binding to and becoming infected with the virus via ACE2 or, alternatively, as professional phagocytes (Silva and Correia-Neves, 2012; Uribe-Querol and Rosales, 2020), are engulfing the invading pathogen through innate recognition pathways. Our data supports a high level of expression of ACE2 at the protein level, but not the RNA level in neutrophils; an observation recently reported by Veras and colleagues (Veras et al., 2020c). By using cytochalasin D to breakdown actin filament organization we significantly reduced internalization, supporting a predominant role

for phagocytosis in the internalization of SARS-CoV-2 in neutrophils, potentially stimulating the increased pro-inflammatory response observed in the co-culture (**Fig. 2**). However, reports are emerging suggesting a significant role for cytoskeletal rearrangement in SARS-CoV-2 entry and, therefore, we cannot entirely rule out infection (Wen et al., 2020). The use of blocking antibodies has potential to elucidate the mechanisms of internalization, however, would pose significant challenges. Neutrophils famously express copious amounts of Fc receptors (Wang and Jonsson, 2019). By including antibodies sensitive or otherwise to present antigens in neutrophil cultures would opsonize any present antigens and be recognized by the neutrophils eventually becoming internalized via opsonized mediated phagocytosis. Indeed, we might likely expect increased internalization with the presence of any antigen sensitive antibodies.

In conclusion, we have developed a model to study neutrophil-epithelial interactions which more closely reflects an *in vivo* and more clinically relevant infection of airways in severe COVID-19 cases than do monocultures. Our findings demonstrate that the co-presence of neutrophils with conducting airway epithelium significantly augments SARS-CoV-2 mediated, pro-inflammatory cytokine release from the epithelium, decreases barrier integrity and increases viral load in the epithelium (summarized in **Fig 5**). Overall, we make important observations that reveal a key role for neutrophil-epithelial interactions in determining infectivity and outcomes in response to SARS-CoV-2 infection that highlight neutrophils as a potential target for prevention of severe COVID-19 disease.

Acknowledgements

The authors acknowledge the Center for Advanced Research Computing (CARC) at the University of Southern California for providing computing resources that have contributed to the research results reported within this publication. URL: https://carc.usc.edu. All Biosafety Level 3 work was performed within The Hastings Foundation and The Wright Foundation Laboratories at USC. SARS-V2 BSL3 resources supported by a grant from the COVID-19 Keck Research Fund, under Lucio Comai. Flow cytometry was performed in the USC Flow Cytometry Facility supported in part by the National Cancer Institute Cancer Center Shared Grant award P30CA014089 and the USC Office of the Provost, Dean's Development Funds, Keck School of Medicine of USC. The content is solely the responsibility of the authors and does not necessarily represent the official views of the National Cancer Institute or the National Institutes of Health. We thank the organ donors and their families for their invaluable donation and the International Institute for the Advancement of Medicine (IIAM), Drs Daniel Weiss and Sharon Mount and the UVMMC autopsy service at the University of Vermont, and Dr. Scott Randell at the University of North Carolina Marsico Lung Institute Tissue Procurement and Cell Culture Core supported in part by NIH DK065988 and grant BOUCHR19R0 from the Cystic Fibrosis Foundation, for their partnership in providing lung tissues for research. Finally, the authors wish to thank the USC COVID-19 Biospecimen Repository for assistance with pathologic analysis

Funding

ALR is funded by the Hastings Foundation, Daniel Tyler Foundation, and the Cystic Fibrosis Foundation (CFFT17XX0 and CFFT21XX0).

Author Contributions

Conceptualization, B.A.C and A.L.R.; Methodology; B.A.C and A.L.R.; Formal Analysis, M.P.S.; Investigation, B.A.C, E.J.Q, Z.L., N.D., C.N.S., S.K., W.D.W., J.E.H., and A.L.R; Writing - Original Draft, B.A.C and A.L.R., Writing – Review and editing, B.A.C and A.L.R., Funding Acquisition, A.L.R.

Declaration of Interests

The authors declare no competing interests

Figures and Figure Legends

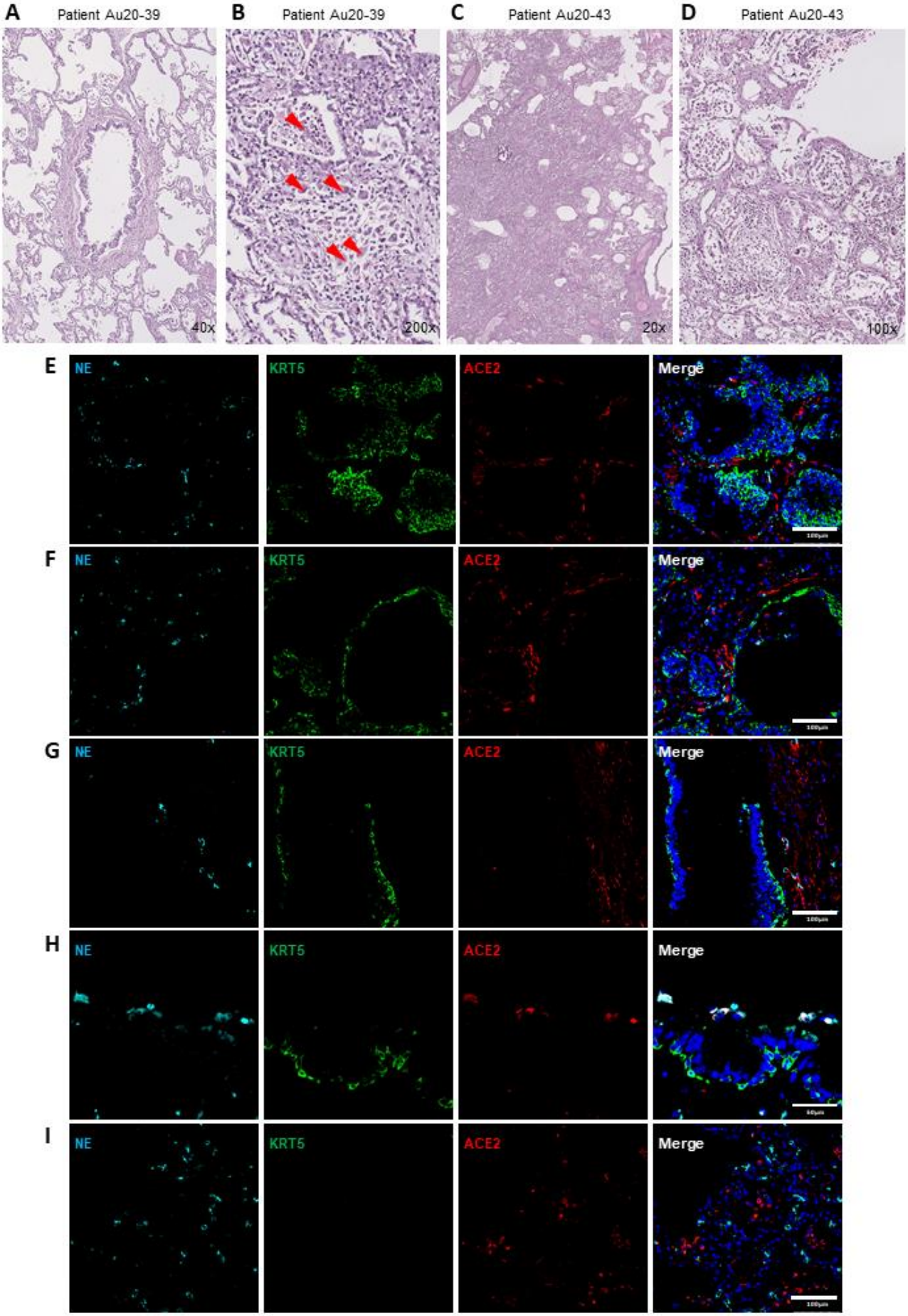
A
Patient Au20-39
40x
B
Patient Au20-39
200x
C
Patient Au20-43
20x
D
Patient Au20-43
100x
E
NE
KRT5
ACE2
Merge
F
NE
KRT5
ACE2
Merge
G
NE
KRT5
ACE2
Merge
H
NE
KRT5
ACE2
Merge
I
NE
KRT5
ACE2
Merge

543

Figure 1: Neutrophil associated tissue pathology in post-mortem COVID19 human lung airways. (A-D) Representative images of hematoxylin and eosin (H&E) staining of postmortem COVID-19 patient tissues showing patchy organizing pneumonia centered around a major artery and an airway (A); focally expanded interstitium by a mixed cellular infiltrate including scattered giant cells (orange arrowheads) (B); diffuse alveolar damage from intense fibroinflammatory process and barotrauma induced rounded airspaces (C) and organizing diffuse alveolar damage with fibrin disposition replaced by organizing pneumonia, inflammatory cells and oedema (D). (E-H) Representative IF images of postmortem COVID-19 tissue probed for NE (cyan), KRT5 (green) and ACE2 (red). Images highlight; small airway occlusion resulting from basal cell hyperplasia with surrounding neutrophils present (E); epithelial damage with breaching neutrophils into the luminal space (F); epithelial shedding, inclusive of basal cell layer with neutrophil inclusion of mucosal surface (G); neutrophil breach into airway luminal space with high neutrophil elastase activity (H) and diffuse neutrophil invasion of alveolar spaces (I). All IF images have nuclei counterstained with DAPI (blue) and scale bars represent 100 µm. All images are representative of 3 independent regions per donor at least 2 independent donors.

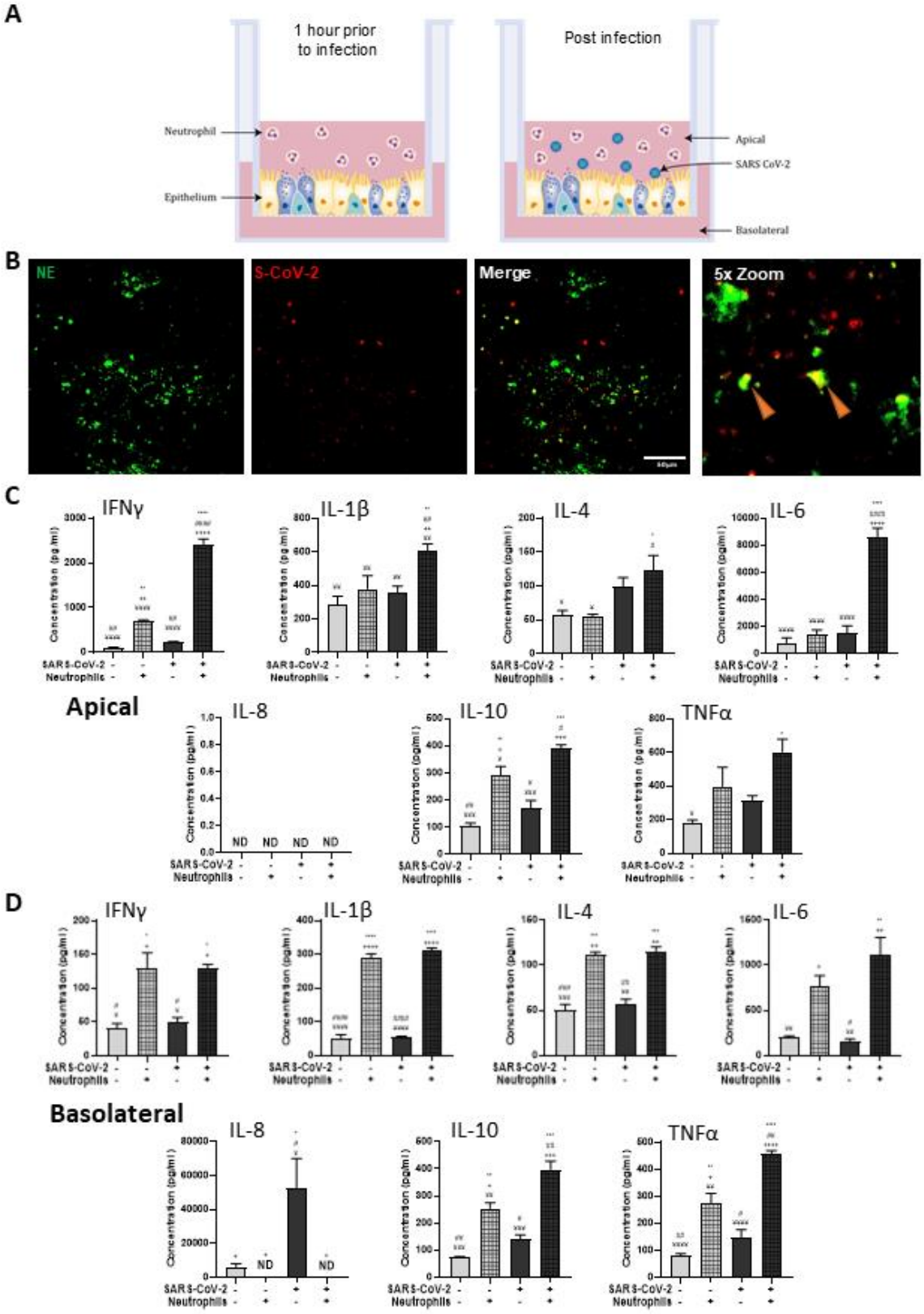
A
1 hour prior to infection
Post infection
Neutrophil
Epithelium
Apical
SARS CoV-2
Basolateral
B
NE
S-CoV-2
Merge
5x Zoom
C
IFNγ
IL-1β
IL-4
IL-6
Concentration (pg/ml)
SARS-CoV-2
Neutrophils
Apical
IL-8
IL-10
TNFα
ND
D
Basolateral

559

Figure 2: Polarized inflammatory response of neutrophils in co-culture with human airway epithelium, infected with SARS-CoV-2. (A) Schematic of the *in vitro* model of neutrophilic airways denoting neutrophils in co-culture with differentiated airway epithelial cells and infected with live SARS-CoV-2 virus. (B) Representative IF images of primary human airway epithelial cells differentiated at the air-liquid interface stained with NE (green) and probed by RNAScope for SARS-CoV-2 (red). Scale bars represent 100μm. Inflammatory profiles of apical (C) and basolateral (D) supernatants collected 4 hours post infection in the neutrophilic airway model. Data is expressed as mean±SEM and significance is determined by analysis of variance (ANOVA) followed by Tukey's post hoc analysis. * compared to uninfected epithelial monoculture, $^{\#}$ compared to uninfected epithelial and neutrophil co-culture, $^{+}$ compared to infected monoculture epithelial cells, ¥ significant from infected neutrophil and epithelial co-culture. *p<0.05,**p<0.01, ***p<0.001, ****,<0.0001 from n=3 experimental repeats from N=3 donors.

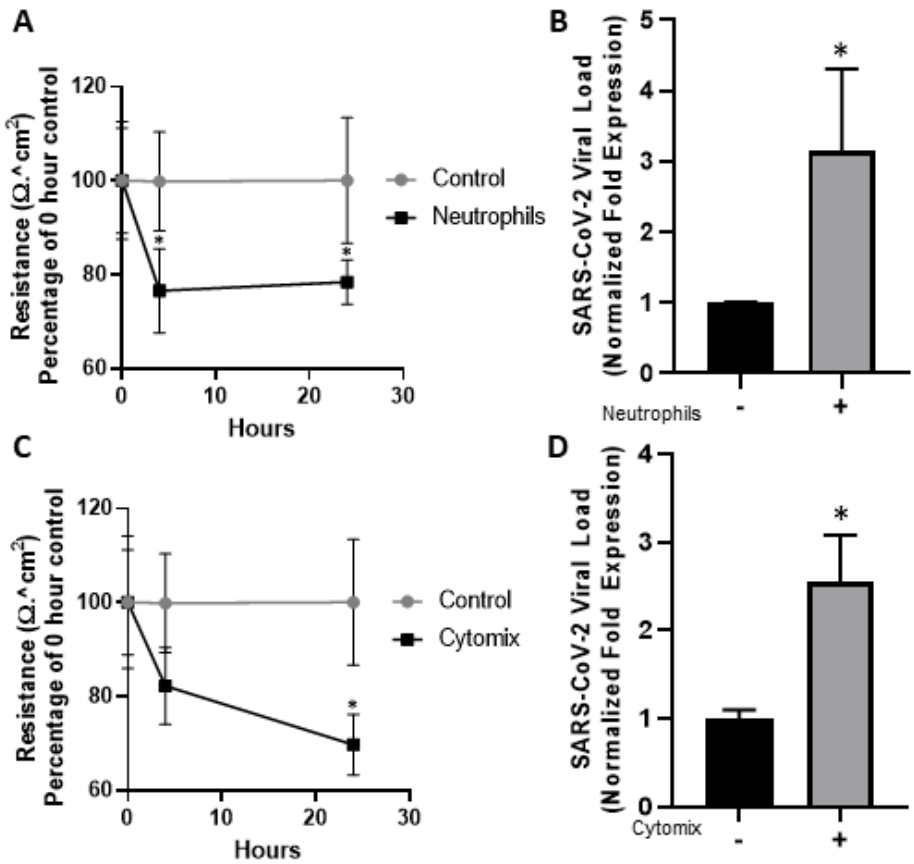

Figure 3: Neutrophils and pro-inflammatory cytokines break down the epithelial barrier and increase viral load in human airway epithelial cells. (A) TEER of human differentiated airway epithelial cells in the presence, or absence (control), of neutrophils. (B) Viral load of SARS-CoV-2 RNA isolated from infected human airway epithelial cells. (C) TEER of human differentiated airway epithelial cells cultured with a "cytomix" of TNFα, IL-1β, IL-6 and IFN-γ each at 10ng/ml. (D) Viral load of SARS-CoV-2 in airway epithelial cells cultured with cytomix. Data are expressed as mean±SEM. Statistical significance of TEER data was determined by ANOVA and viral load data was analyzed using an unpaired two-tailed Student's t-test. *$p<0.05$. Experiments include N=3 independent epithelial donors paired with N=3 independent neutrophil donors.

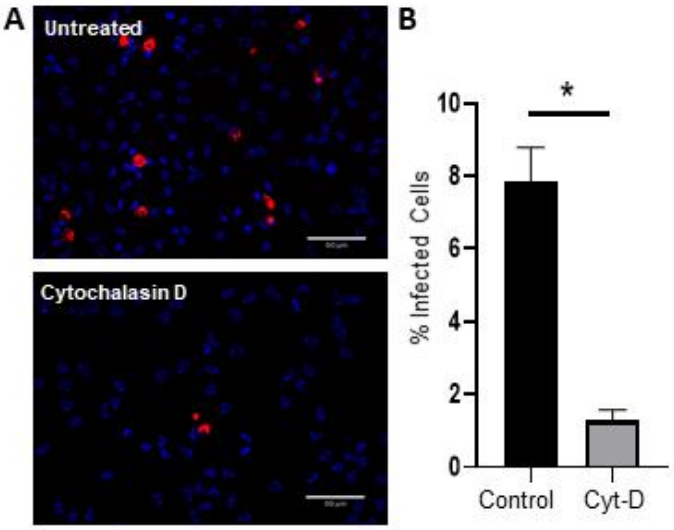

Figure 4. Cytochalasin D inhibits internalization of SARS-CoV-2 in neutrophils. (A) Representative IF images of neutrophils infected with SARS-CoV-2 (red) detected by RNAScope. (B) Quantification or SARS-CoV-2 positive neutrophils relative to total number of neutrophils determined by DAPI (blue). Data expressed as mean±SEM. **p<0.01 unpaired 2-tailed Student's T-test. N=3 independent neutrophil donors, n=2 experimental replicates.

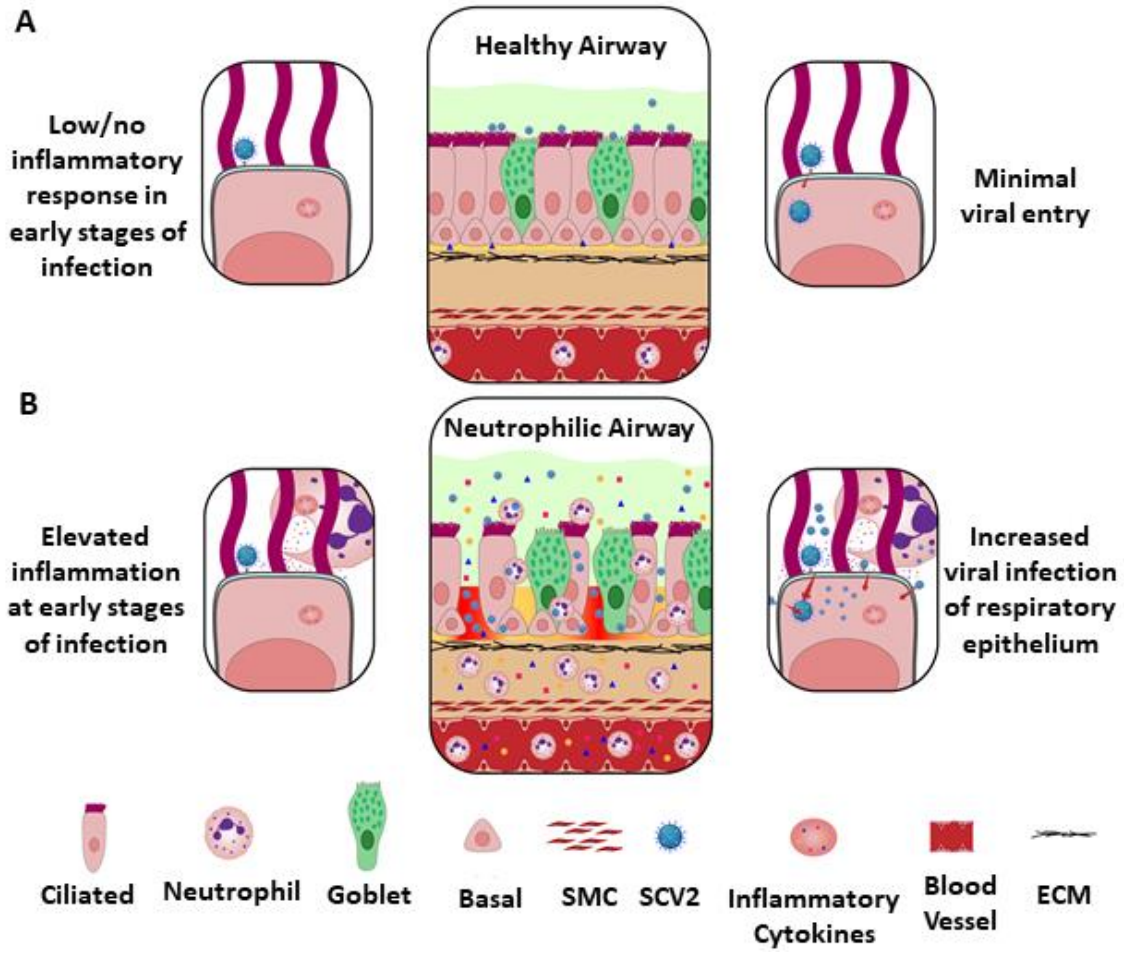

Figure 5: Chronic airway neutrophilia enhances airway inflammation and viral load in response to SARS-CoV-2. Schematic depicting the immediate impact of SARS-CoV-2 on the respiratory epithelium. (A) In a healthy airway with little to no pre-existing inflammation there is minimal inflammatory response and low detection of viral entry to the proximal airway epithelium in the early stages of response to SARS-CoV-2 infection. (B) Where chronic inflammation is pre-existing, for example in the case of many SARS-CoV-2 comorbidities, a significantly enhanced and immediate inflammatory response is observed which correlates with increased infection of the respiratory epithelium and a decrease in barrier integrity. ECM (extracellular matrix), SVC2 (SARS-CoV-2), SMC (smooth muscle cell)

References

Al-Sadi, R., Boivin, M., and Ma, T. (2009). Mechanism of cytokine modulation of epithelial tight junction barrier. Front Biosci (Landmark Ed) *14*, 2765-2778.

Arcanjo, A., Logullo, J., Menezes, C.C.B., de Souza Carvalho Giangiarulo, T.C., Dos Reis, M.C., de Castro, G.M.M., da Silva Fontes, Y., Todeschini, A.R., Freire-de-Lima, L., Decote-Ricardo, D.*, et al.* (2020). The emerging role of neutrophil extracellular traps in severe acute respiratory syndrome coronavirus 2 (COVID-19). Sci Rep *10*, 19630.

Aveyard, P., Gao, M., Lindson, N., Hartmann-Boyce, J., Watkinson, P., Young, D., Coupland, C.A.C., Tan, P.S., Clift, A.K., Harrison, D.*, et al.* (2021). Association between pre-existing respiratory disease and its treatment, and severe COVID-19: a population cohort study. Lancet Respir Med.

Azevedo, M.L.V., Zanchettin, A.C., Vaz de Paula, C.B., Motta Junior, J.D.S., Malaquias, M.A.S., Raboni, S.M., Neto, P.C., Zeni, R.C., Prokopenko, A., Borges, N.H.*, et al.* (2021). Lung Neutrophilic Recruitment and IL-8/IL-17A Tissue Expression in COVID-19. Front Immunol *12*, 656350.

Baggiolini, M., Walz, A., and Kunkel, S.L. (1989). Neutrophil-activating peptide-1/interleukin 8, a novel cytokine that activates neutrophils. J Clin Invest *84*, 1045-1049.

Bordon, J., Aliberti, S., Fernandez-Botran, R., Uriarte, S.M., Rane, M.J., Duvvuri, P., Peyrani, P., Morlacchi, L.C., Blasi, F., and Ramirez, J.A. (2013). Understanding the roles of cytokines and neutrophil activity and neutrophil apoptosis in the protective versus deleterious inflammatory response in pneumonia. Int J Infect Dis *17*, e76-83.

Borges, L., Pithon-Curi, T.C., Curi, R., and Hatanaka, E. (2020). COVID-19 and Neutrophils: The Relationship between Hyperinflammation and Neutrophil Extracellular Traps. Mediators Inflamm *2020*, 8829674.

Capaldo, C.T., and Nusrat, A. (2009). Cytokine regulation of tight junctions. Biochim Biophys Acta *1788*, 864-871.

Carraro, G., Langerman, J., Sabri, S., Lorenzana, Z., Purkayastha, A., Zhang, G., Konda, B., Aros, C.J., Calvert, B.A., Szymaniak, A.*, et al.* (2021). Transcriptional analysis of cystic fibrosis airways at single-cell resolution reveals altered epithelial cell states and composition. Nat Med *27*, 806-814.

Chen, G., Wu, D., Guo, W., Cao, Y., Huang, D., Wang, H., Wang, T., Zhang, X., Chen, H., Yu, H.*, et al.* (2020). Clinical and immunological features of severe and moderate coronavirus disease 2019. J Clin Invest *130*, 2620-2629.

Chen, M.M., Palmer, J.L., Plackett, T.P., Deburghgraeve, C.R., and Kovacs, E.J. (2014). Age-related differences in the neutrophil response to pulmonary pseudomonas infection. Exp Gerontol *54*, 42-46.

Corteling, R., Wyss, D., and Trifilieff, A. (2002). In vivo models of lung neutrophil activation. Comparison of mice and hamsters. BMC Pharmacol *2*, 1.

Del Valle, D.M., Kim-Schulze, S., Huang, H.H., Beckmann, N.D., Nirenberg, S., Wang, B., Lavin, Y., Swartz, T.H., Madduri, D., Stock, A.*, et al.* (2020). An inflammatory cytokine signature predicts COVID-19 severity and survival. Nat Med *26*, 1636-1643.

Fahlberg, M.D., Blair, R.V., Doyle-Meyers, L.A., Midkiff, C.C., Zenere, G., Russell-Lodrigue, K.E., Monjure, C.J., Haupt, E.H., Penney, T.P., Lehmicke, G.*, et al.* (2020). Cellular events of acute, resolving or progressive COVID-19 in SARS-CoV-2 infected non-human primates. Nat Commun *11*, 6078.

Fajgenbaum, D.C., and June, C.H. (2020). Cytokine Storm. N Engl J Med *383*, 2255-2273.

Florentin, J., Zhao, J., Tai, Y.Y., Vasamsetti, S.B., O'Neil, S.P., Kumar, R., Arunkumar, A., Watson, A., Sembrat, J., Bullock, G.C.*, et al.* (2021). Interleukin-6 mediates neutrophil mobilization from bone marrow in pulmonary hypertension. Cell Mol Immunol *18*, 374-384.

Galani, I.E., and Andreakos, E. (2015). Neutrophils in viral infections: Current concepts and caveats. J Leukoc Biol *98*, 557-564.

Gernez, Y., Tirouvanziam, R., and Chanez, P. (2010). Neutrophils in chronic inflammatory airway diseases: can we target them and how? Eur Respir J *35*, 467-469.

Godkin, A., and Humphreys, I.R. (2020). Elevated interleukin-6, interleukin-10 and neutrophil : lymphocyte ratio as identifiers of severe coronavirus disease 2019. Immunology *160*, 221-222.

Grommes, J., and Soehnlein, O. (2011). Contribution of neutrophils to acute lung injury. Mol Med *17*, 293-307.

Guan, W.J., Ni, Z.Y., Hu, Y., Liang, W.H., Ou, C.Q., He, J.X., Liu, L., Shan, H., Lei, C.L., Hui, D.S.C.*, et al.* (2020). Clinical Characteristics of Coronavirus Disease 2019 in China. N Engl J Med *382*, 1708-1720.

Han, H., Ma, Q., Li, C., Liu, R., Zhao, L., Wang, W., Zhang, P., Liu, X., Gao, G., Liu, F.*, et al.* (2020). Profiling serum cytokines in COVID-19 patients reveals IL-6 and IL-10 are disease severity predictors. Emerg Microbes Infect *9*, 1123-1130.

Hemmat, N., Derakhshani, A., Bannazadeh Baghi, H., Silvestris, N., Baradaran, B., and De Summa, S. (2020). Neutrophils, Crucial, or Harmful Immune Cells Involved in Coronavirus Infection: A Bioinformatics Study. Frontiers in genetics *11*, 641.

Huang, C., Wang, Y., Li, X., Ren, L., Zhao, J., Hu, Y., Zhang, L., Fan, G., Xu, J., Gu, X.*, et al.* (2020a). Clinical features of patients infected with 2019 novel coronavirus in Wuhan, China. Lancet *395*, 497-506.

Huang, H., Zhang, M., Chen, C., Zhang, H., Wei, Y., Tian, J., Shang, J., Deng, Y., Du, A., and Dai, H. (2020b). Clinical characteristics of COVID-19 in patients with preexisting ILD: A retrospective study in a single center in Wuhan, China. J Med Virol *92*, 2742-2750.

Janiuk, K., Jablonska, E., and Garley, M. (2021). Significance of NETs Formation in COVID-19. Cells *10*.

Jasper, A.E., McIver, W.J., Sapey, E., and Walton, G.M. (2019). Understanding the role of neutrophils in chronic inflammatory airway disease. F1000Res *8*.

Jia, H.P., Look, D.C., Shi, L., Hickey, M., Pewe, L., Netland, J., Farzan, M., Wohlford-Lenane, C., Perlman, S., and McCray, P.B., Jr. (2005). ACE2 receptor expression and severe acute respiratory syndrome coronavirus infection depend on differentiation of human airway epithelia. J Virol *79*, 14614-14621.

Jia, H.P., Look, D.C., Tan, P., Shi, L., Hickey, M., Gakhar, L., Chappell, M.C., Wohlford-Lenane, C., and McCray, P.B., Jr. (2009). Ectodomain shedding of angiotensin converting enzyme 2 in human airway epithelia. Am J Physiol Lung Cell Mol Physiol *297*, L84-96.

Kordonowy, L.L., Burg, E., Lenox, C.C., Gauthier, L.M., Petty, J.M., Antkowiak, M., Palvinskaya, T., Ubags, N., Rincon, M., Dixon, A.E.*, et al.* (2012). Obesity is associated with neutrophil dysfunction and attenuation of murine acute lung injury. Am J Respir Cell Mol Biol *47*, 120-127.

Kulkarni, U., Zemans, R.L., Smith, C.A., Wood, S.C., Deng, J.C., and Goldstein, D.R. (2019). Excessive neutrophil levels in the lung underlie the age-associated increase in influenza mortality. Mucosal Immunol *12*, 545-554.

Kumar, S., Yadav, P.K., Srinivasan, R., and Perumal, N. (2020). Selection of animal models for COVID-19 research. Virusdisease, 1-6.

Kunkel, S.L., Standiford, T., Kasahara, K., and Strieter, R.M. (1991). Interleukin-8 (IL-8): the major neutrophil chemotactic factor in the lung. Exp Lung Res *17*, 17-23.

Li, G., He, X., Zhang, L., Ran, Q., Wang, J., Xiong, A., Wu, D., Chen, F., Sun, J., and Chang, C. (2020). Assessing ACE2 expression patterns in lung tissues in the pathogenesis of COVID-19. J Autoimmun *112*, 102463.

Liu, J., Li, S., Liu, J., Liang, B., Wang, X., Wang, H., Li, W., Tong, Q., Yi, J., Zhao, L.*, et al.* (2020a). Longitudinal characteristics of lymphocyte responses and cytokine profiles in the peripheral blood of SARS-CoV-2 infected patients. EBioMedicine *55*, 102763.

Liu, Q.Q., Cheng, A., Wang, Y., Li, H., Hu, L., Zhao, X., Wang, T., and He, F. (2020b). Cytokines and their relationship with the severity and prognosis of coronavirus disease 2019 (COVID-19): a retrospective cohort study. BMJ Open *10*, e041471.

Maia, L.A., Cruz, F.F., de Oliveira, M.V., Samary, C.S., Fernandes, M.V.S., Trivelin, S.A.A., Rocha, N.N., Gama de Abreu, M., Pelosi, P., Silva, P.L.*, et al.* (2019). Effects of Obesity on Pulmonary Inflammation and Remodeling in Experimental Moderate Acute Lung Injury. Front Immunol *10*, 1215.

Manicone, A.M., Gong, K., Johnston, L.K., and Giannandrea, M. (2016). Diet-induced obesity alters myeloid cell populations in naive and injured lung. Respir Res *17*, 24.

Monchatre-Leroy, E., Lesellier, S., Wasniewski, M., Picard-Meyer, E., Richomme, C., Boue, F., Lacote, S., Murri, S., Pulido, C., Vulin, J.*, et al.* (2021). Hamster and ferret experimental infection with intranasal low dose of a single strain of SARS-CoV-2. J Gen Virol *102*.

Monchatre-Leroy, E., Lesellier, S., Wasniewski, M., Picard-Meyer, E., Richomme, C., Boué, F., Lacôte, S., Murri, S., Pulido, C., Vulin, J.*, et al.* (2020). Hamster and ferret experimental infection with intranasal low dose of a single strain of SARS-CoV-2. bioRxiv, 2020.2009.2024.311977.

Munoz-Fontela, C., Dowling, W.E., Funnell, S.G.P., Gsell, P.S., Riveros-Balta, A.X., Albrecht, R.A., Andersen, H., Baric, R.S., Carroll, M.W., Cavaleri, M.*, et al.* (2020). Animal models for COVID-19. Nature *586*, 509-515.

Pandolfi, L., Fossali, T., Frangipane, V., Bozzini, S., Morosini, M., D'Amato, M., Lettieri, S., Urtis, M., Di Toro, A., Saracino, L.*, et al.* (2020). Broncho-alveolar inflammation in COVID-19 patients: a correlation with clinical outcome. BMC Pulm Med *20*, 301.

Parkos, C.A. (2016). Neutrophil-Epithelial Interactions: A Double-Edged Sword. Am J Pathol *186*, 1404-1416.

Parsons, P.E., Fowler, A.A., Hyers, T.M., and Henson, P.M. (1985). Chemotactic activity in bronchoalveolar lavage fluid from patients with adult respiratory distress syndrome. Am Rev Respir Dis *132*, 490-493.

Pease, J.E., and Sabroe, I. (2002). The role of interleukin-8 and its receptors in inflammatory lung disease: implications for therapy. Am J Respir Med *1*, 19-25.

Pechous, R.D. (2017). With Friends Like These: The Complex Role of Neutrophils in the Progression of Severe Pneumonia. Front Cell Infect Microbiol *7*, 160.

Pfaffl, M.W. (2001). A new mathematical model for relative quantification in real-time RT-PCR. Nucleic Acids Res *29*, e45.

Qin, C., Zhou, L., Hu, Z., Zhang, S., Yang, S., Tao, Y., Xie, C., Ma, K., Shang, K., Wang, W.*, et al.* (2020). Dysregulation of Immune Response in Patients With Coronavirus 2019 (COVID-19) in Wuhan, China. Clinical infectious diseases : an official publication of the Infectious Diseases Society of America *71*, 762-768.

Qun, S., Wang, Y., Chen, J., Huang, X., Guo, H., Lu, Z., Wang, J., Zheng, C., Ma, Y., Zhu, Y.*, et al.* (2020). Neutrophil-to-Lymphocyte Ratios Are Closely Associated With the Severity and Course of Non-mild COVID-19. Front Immunol *11*, 2160.

Radermecker, C., Sabatel, C., Vanwinge, C., Ruscitti, C., Marechal, P., Perin, F., Schyns, J., Rocks, N., Toussaint, M., Cataldo, D.*, et al.* (2019). Locally instructed CXCR4(hi) neutrophils trigger environment-driven allergic asthma through the release of neutrophil extracellular traps. Nat Immunol *20*, 1444-1455.

Randell, S.H., Walstad, L., Schwab, U.E., Grubb, B.R., and Yankaskas, J.R. (2001). Isolation and culture of airway epithelial cells from chronically infected human lungs. In Vitro Cell Dev Biol Anim *37*, 480-489.

Ruan, Q., Yang, K., Wang, W., Jiang, L., and Song, J. (2020). Correction to: Clinical predictors of mortality due to COVID-19 based on an analysis of data of 150 patients from Wuhan, China. Intensive Care Med *46*, 1294-1297.

Ryan, K.A., Bewley, K.R., Fotheringham, S.A., Slack, G.S., Brown, P., Hall, Y., Wand, N.I., Marriott, A.C., Cavell, B.E., Tree, J.A.*, et al.* (2021). Dose-dependent response to infection with SARS-CoV-2 in the ferret model and evidence of protective immunity. Nat Commun *12*, 81.

Sapey, E., Patel, J.M., Greenwood, H.L., Walton, G.M., Hazeldine, J., Sadhra, C., Parekh, D., Dancer, R.C.A., Nightingale, P., Lord, J.M.*, et al.* (2017). Pulmonary Infections in the Elderly Lead to Impaired Neutrophil Targeting, Which Is Improved by Simvastatin. Am J Respir Crit Care Med *196*, 1325-1336.

Shi, H., Zuo, Y., Yalavarthi, S., Gockman, K., Zuo, M., Madison, J.A., Blair, C.N., Woodard, W., Lezak, S.P., Lugogo, N.L.*, et al.* (2020). Neutrophil calprotectin identifies severe pulmonary disease in COVID-19. medRxiv : the preprint server for health sciences.

Silva, M.T., and Correia-Neves, M. (2012). Neutrophils and macrophages: the main partners of phagocyte cell systems. Front Immunol *3*, 174.

Song, C.-Y., Xu, J., He, J.-Q., and Lu, Y.-Q. (2020). COVID-19 early warning score: a multi-parameter screening tool to identify highly suspected patients. medRxiv, 2020.2003.2005.20031906.

Stackowicz, J., Jonsson, F., and Reber, L.L. (2019). Mouse Models and Tools for the in vivo Study of Neutrophils. Front Immunol *10*, 3130.

Taylor, S., Dirir, O., Zamanian, R.T., Rabinovitch, M., and Thompson, A.A.R. (2018). The Role of Neutrophils and Neutrophil Elastase in Pulmonary Arterial Hypertension. Front Med (Lausanne) *5*, 217.

Thomson, G.A., Fisher, B.M., Gemmell, C.G., MacCuish, A.C., and Gallacher, S.J. (1997). Attenuated neutrophil respiratory burst following acute hypoglycaemia in diabetic patients and normal subjects. Acta Diabetol *34*, 253-256.

Tomar, B., Anders, H.J., Desai, J., and Mulay, S.R. (2020). Neutrophils and Neutrophil Extracellular Traps Drive Necroinflammation in COVID-19. Cells *9*.

Uribe-Querol, E., and Rosales, C. (2020). Phagocytosis: Our Current Understanding of a Universal Biological Process. Front Immunol *11*, 1066.

Veras, F.P., Pontelli, M., Silva, C., Toller-Kawahisa, J., de Lima, M., Nascimento, D., Schneider, A., Caetite, D., Rosales, R., Colon, D.*, et al.* (2020a). SARS-CoV-2 triggered neutrophil extracellular traps (NETs) mediate COVID-19 pathology. medRxiv : the preprint server for health sciences, 2020.2006.2008.20125823.

Veras, F.P., Pontelli, M.C., Silva, C.M., Toller-Kawahisa, J.E., de Lima, M., Nascimento, D.C., Schneider, A.H., Caetite, D., Tavares, L.A., Paiva, I.M.*, et al.* (2020b). SARS-CoV-2-triggered neutrophil extracellular traps mediate COVID-19 pathology. J Exp Med *217*.

Veras, F.P., Pontelli, M.C., Silva, C.M., Toller-Kawahisa, J.E., de Lima, M., Nascimento, D.C., Schneider, A.H., Caetité, D., Tavares, L.A., Paiva, I.M.*, et al.* (2020c). SARS-CoV-2–triggered neutrophil extracellular traps mediate COVID-19 pathology. Journal of Experimental Medicine *217*.

Wang, Y., and Jonsson, F. (2019). Expression, Role, and Regulation of Neutrophil Fcgamma Receptors. Front Immunol *10*, 1958.

Wen, Z., Zhang, Y., Lin, Z., Shi, K., and Jiu, Y. (2020). Cytoskeleton-a crucial key in host cell for coronavirus infection. J Mol Cell Biol *12*, 968-979.

Wu, Z., and McGoogan, J.M. (2020). Characteristics of and Important Lessons From the Coronavirus Disease 2019 (COVID-19) Outbreak in China: Summary of a Report of 72314 Cases From the Chinese Center for Disease Control and Prevention. JAMA *323*, 1239-1242.

Yang, P.H., Ding, Y.B., Xu, Z., Pu, R., Li, P., Yan, J., Liu, J.L., Meng, F.P., Huang, L., Shi, L.*, et al.* (2020). Increased circulating level of interleukin-6 and CD8(+) T cell exhaustion are associated with progression of COVID-19. Infect Dis Poverty *9*, 161.

Yoshimura, T., Matsushima, K., Tanaka, S., Robinson, E.A., Appella, E., Oppenheim, J.J., and Leonard, E.J. (1987). Purification of a human monocyte-derived neutrophil chemotactic factor that has peptide sequence similarity to other host defense cytokines. Proc Natl Acad Sci U S A *84*, 9233-9237.

Zhang, B., Zhou, X., Zhu, C., Song, Y., Feng, F., Qiu, Y., Feng, J., Jia, Q., Song, Q., Zhu, B.*, et al.* (2020a). Immune Phenotyping Based on the Neutrophil-to-Lymphocyte Ratio and IgG Level Predicts Disease Severity and Outcome for Patients With COVID-19. Front Mol Biosci *7*, 157.

Zhang, H., Rostami, M.R., Leopold, P.L., Mezey, J.G., O'Beirne, S.L., Strulovici-Barel, Y., and Crystal, R.G. (2020b). Expression of the SARS-CoV-2 ACE2 Receptor in the Human Airway Epithelium. Am J Respir Crit Care Med *202*, 219-229.

Zhu, C., Yu, S., Zhao, H., Shen, H., Yang, J., Zhao, L., and Wu, W. (2020a). Neutrophil-to-lymphocyte ratio predicts the clearance of SARS-CoV-2 RNA in mild COVID-19 patients - a retrospective analysis from Dongxihu Fangcang Hospital in Wuhan, China. Clin Chem Lab Med *58*, e167-e170.

Zhu, N., Wang, W., Liu, Z., Liang, C., Wang, W., Ye, F., Huang, B., Zhao, L., Wang, H., Zhou, W.*, et al.* (2020b). Morphogenesis and cytopathic effect of SARS-CoV-2 infection in human airway epithelial cells. Nat Commun *11*, 3910.